Northeastern University Probing Regolith Ice-Extracting System for Mars and the Moon (PRISMM)

NASA RASC-AL Moon to Mars Ice & Prospecting Challenge 2020

Advisor: Professor Taskin Padir

Authors: Samuel Hibbard (1st Year Mechanical Eng.)

Ethan Holand (1st Year Mechanical Eng.)

Jarrod Homer (1st Year Electrical Eng.)

Christian Burwell (1st Year Electrical & Computer Eng.)

Maulik Patel (1st Year Electrical Eng.)

Smeet Patel (1st Year Mechanical Eng.)

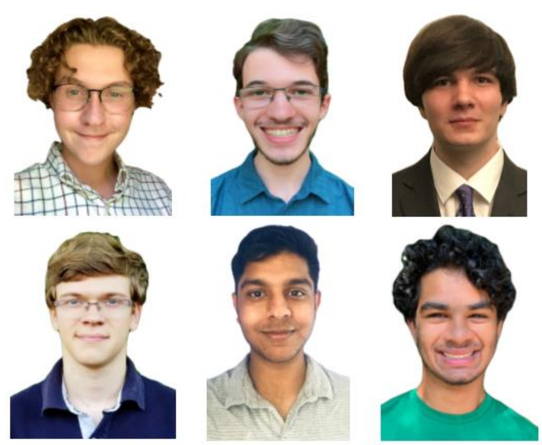

Table of Contents

Nomenclature

PRISMM	Probing Regolith Ice-Extracting System for Mars and the Moon
RAPID	the Rotary and Percussive Instrument for Drilling
WOB	Weight on Bit
HMM	Hidden Markov Model
MET	the Melting and Extracting Tool
ROS	Robot Operating System
OBC	Onboard Computer
GSC	Ground Station Computer
RTG	Radioisotope Thermoelectric Generator

1 Executive Summary

1.1 Introduction

The Northeastern University **P**robing **R**egolith **I**ce-Extracting **S**ystem for **M**ars and the **M**oon (PRISMM) is a robotic system designed to extract available subsurface ice and provide geological insight about the Moon and Mars. The system was developed within the design objectives and constraints set by NASA's 2020 RASC-AL Moon to Mars Ice and Prospecting Challenge. Overcoming this challenge is vital, as in-situ resource utilization on other planetary bodies is paramount for extraterrestrial exploration and expansion.

1.2 Drilling Operations

PRISMM bores through simulated extraterrestrial terrain via the **R**otary **a**nd **P**ercussive **I**nstrument for **D**rilling (RAPID) equipped with a concrete-optimized auger. Information about overburden layers is gathered via a pair of load cells, a custom Hall effect encoder, and a current draw sensor.

1.3 Digital Core Prospecting

PRISMM synthesizes a digital core by measuring metrics including **w**eight **o**n **b**it (WOB), r/min, drill position, and time. Accuracy can be maximized via a **H**idden **M**arkov **M**odel (HMM) and pseudo-Rockwell hardness testing. Additionally, a new metric, pseudo-average impulse per mm, can be used to estimate the relative hardness of each layer.

1.4 Water Extraction

After reaching ice, the tool rack shifts to insert the **M**elting and **E**xtracting **T**ool (MET). It descends until a limit switch detects it has reached the bottom surface. A custom heating probe fixed to the end of MET's meter-long shaft begins melting the surrounding ice via four cartridge heaters. Servos housed at the top of MET control the heaters' yaw and pitch, allowing 360° of rotation and outwards articulation. As water pools at the bottom of the created spherical sector, it is pumped into the filtration system.

1.5 Water Filtration

The filtration system has four layers. The first is a metal screen at the inlet tube, which prevents the tubing from being clogged by large debris. The second and third layers of filtration are custom regenerative filters that remove mid-sized particles. Next, water passes through a fine 1 µm filter. Finally, water exits into an external accumulation tank. The regenerative filters are autonomously cleaned by recirculating water using purge valves, increasing the system's lifespan.

1.6 Hardware Control

The avionics on PRISMM support a **R**obot **O**perating **S**ystem (ROS) network. This enables peripherals, including sensors and motors, to communicate with higher-level software on a common local area network. To connect the peripherals, three AVR microcontrollers encode and decode sensor data and commands over a serial interface with an **o**n**b**oard **c**omputer (OBC). The OBC acts as PRISMM's central processing unit, managing all communication over the ROS network and handling tasks such as state management and data logging. This allows a **g**round **s**tation **c**omputer (GSC), connected via ethernet, to focus on managing user interfacing with the ROS network.

2 System Description

2.1 Framing

PRISMM's framing system is composed of an H-shaped base with two vertical posts supported by 45° struts (**Fig. 1**). 1.5 in aluminum 80/20 extrusion was chosen for its suitable strength-to-weight ratio and ease of customization. Internal double-anchor fasteners at the ends of each beam provide a vibration-resistant means of joining the frame. Four adjustable L-brackets attached to the base allow the system to be mounted to a testbed by inserting wood screws.

A rectangular tool rack slides horizontally along the frame using four sets of roller wheels. Its two vertical rails carry sliders with separate lead screws run by Nema 23 stepper motors, allowing RAPID and MET to raise and descend independently. The tool rack position can be set by rotating a belt pulley attached to its base, allowing tool swapping and drill relocation.

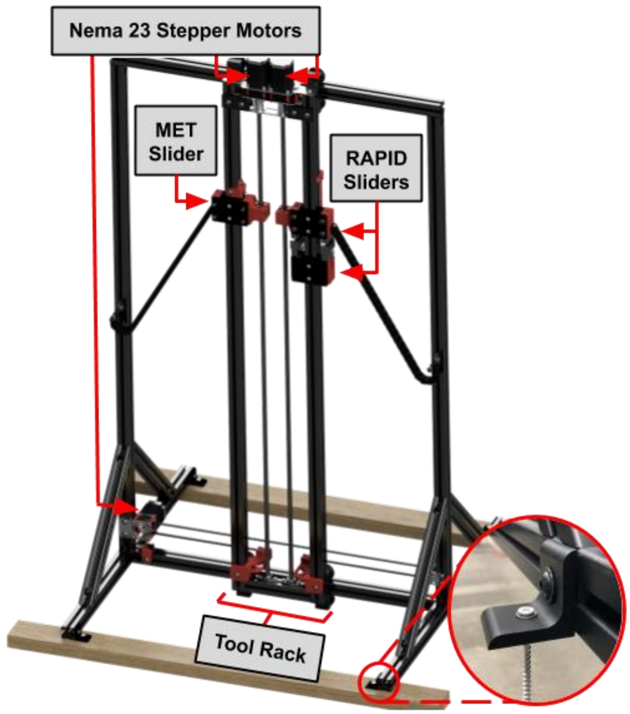

Fig. 1. *PRISMM's framing configuration*

2.2 Excavation Operations

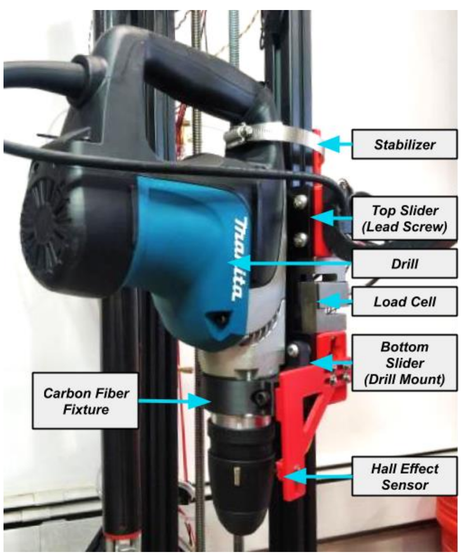

Fig. 2. *RAPID breakdown*

2.2.1 Drilling

RAPID is driven by a Makita HR4002 hammer drill. It uses an auger with a 30-1/2 in working length and a 2-3/16 in bore diameter. Its solid carbide multi-cutter head is optimized for materials with the hardness of reinforced concrete, and its heat-treated flutes draw debris up and out to the surface.

Two sliders are used to mount RAPID to the tool rack. The lower slider contains a custom printed Onyx and carbon fiber reinforced fixture, securely constraining the drill (**Fig. 2**). The upper slider features an adjustable top support for the handle and houses the brass nut that travels along the lead screw. The top and bottom sliders are connected only by a pair of load cells, acting as an intermediary between the force of the bit and force of the lead screw, thus collecting accurate WOB data when summed.

2.2.2 Freezing Mitigation

The drill will never be at rest while below the ice, which should mitigate freezing. Additionally, friction from drilling should produce enough heat to prevent freezing, indicated by previous years' systems and preliminary testing. However, should the drill begin to freeze, the Hall effect sensor can detect declining r/min, and retract RAPID until the temperature starts to balance with the atmosphere. There is much less concern for the heating probe freezing as thermocouples constantly monitor its temperature and adjust the cartridge heaters accordingly. Unfortunately, due to the COVID-19 pandemic, PRISMM's freezing mitigation strategy could not be thoroughly validated.

2.3 Melting and Extraction System

MET consists of an articulating melting arm and an extraction appendage fixed at the end of a meter-long carbon fiber shaft (**Fig. 3**). The carbon fiber shaft rotates on a bearing resting in a pillow block, allowing the tool to pivot 360° along its central axis.

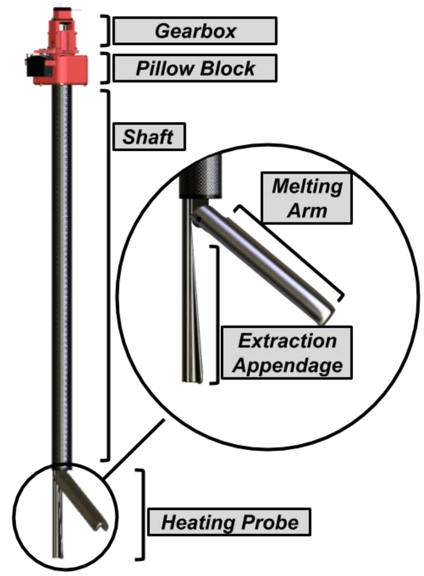

Fig. 3. *MET breakdown*

The melting arm contains four 200 W cartridge heaters and two thermocouples. The heaters are secured in machined aluminum with a thermally conductive metallic epoxy (**Fig. 4**). The extraction appendage consists of an inlet tube, purge tube, and a PETG fixture. This fixture holds a thin rod which activates a limit switch for surface detection and acts as a pivot point. Printed PETG parts were treated with a custom coating to raise their melting point. The coating consists of a high temp epoxy and 20 μm glass microspheres. The microspheres act as an insulator, lowering the thermal conductivity of the epoxy and protecting the plastic. The epoxy also increases the rigidity of the plastic, preventing it from softening. This mixture proved effective in preventing the degradation of printed PETG parts up to 150 °C.

Fig. 4. *Custom machined heating probe*

The pitch of MET is driven by an anchored pulley attached to the melting arm. Wire rope leading up the length of the shaft attaches to another pulley, driven by a 2:1 bevel gear above the pillow block. As MET rotates reciprocally, the melting arm hinges outwards for constant ice contact, forming a bowl-shaped cavity seen in **Fig. 5**.

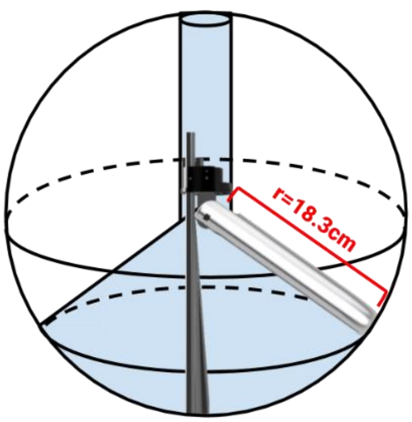

Fig. 5. *The spherical sector melted by MET*

The bowl's volume equals a hemisphere with the radius of the melting arm, which is 18.3 cm. This equates to 25.7 L of ice per bowl, which corresponds to around 23.8 L of water. Given a Martian temperature of -60 °C, and a heating power of 800 W, PRISMM could melt a theoretical maximum of 6.46 L per hour, or a 25.7 L bowl in 3.97 hours. Considering that the ice temperature at the competition is only -10 °C, this increases to 8.18 L per hour. Provided 1 hour of drilling and 11 hours of melting, this could yield 90 L of water. Even if the probe only operated at a fraction of this efficiency, the amount of water obtained would be considerable.

2.4 Filtration and Water Collection

Due to the spheroidal shape of the melted area, all water will pool at the bottom, allowing it to be withdrawn using the side inlet of the extraction appendage. This inlet has a mesh cover and rests 1 cm above the bottom of the bowl, preventing unwanted sediment extraction.

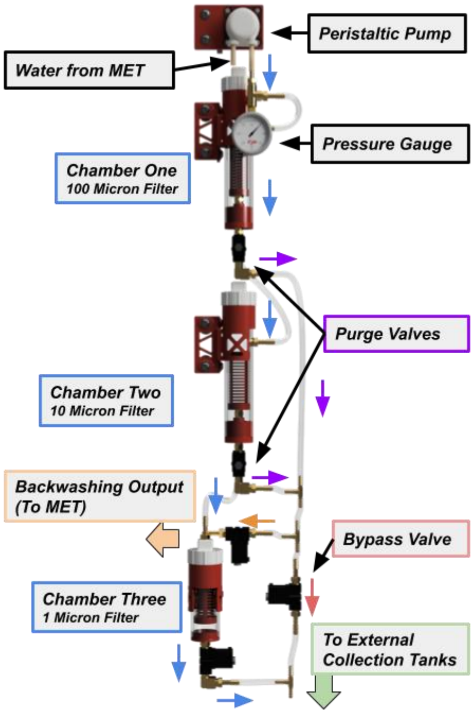

Fig. 6. *Water filtration system*

Given the high power consumption from RAPID and MET, a less demanding system was needed for water filtration. Mesh filters were selected for their significantly lower power usage and mass than alternative methods such as distillation and electroflocculation. PRISMM's filtration system addresses the longevity of traditional mesh systems with its capability of autonomously backwashing filters. **Fig. 6** details the filtration system's different operations.

The filtration system consists of a 280 µm aluminum screen, and a 100 µm nylon filter, followed by 10 and 1 µm felt-coated polypropylene filters. Using four separate filters reduces the amount of build-up in individual parts, allowing for longer use between purging filters and backwashing.

Filtration is run using a 24 V peristaltic pump. The pump consumes less than 36 W and has a pump rate of 160 mL/min. The filtration system is actuated using five electric solenoid valves controlled by relays.

Clogging of the metal screen in the extraction appendage can be remedied by pumping water back down the purge tube. A buildup of material in filter chamber one or two can be removed by opening the purge valves of their respective filters and recirculating the dirty water into the bowl melted by MET. In testing, purging water from chamber one successfully removed the buildup of material from the 100 µm nylon filter. However, in filter chamber two, the outer layer of felt on the filter prevented a significant amount of particulate from being drained away.

A successful test of the filtration system was conducted using a bucket filled with water and roughly 15% dirt by volume. The samples of unfiltered and filtered water can be seen in **Fig. 7**.

Fig. 7. *Unfiltered water (left) vs. filtered water (right)*

2.5 Control and Communication

2.5.1 Electrical

The primary electronics for PRISMM are mounted on an acrylic panel on the back of the system seen in **Fig. 8**. Components are attached using standoffs, screws, and custom 3D printed brackets. Peripherals such as motors, sensors, heaters, and the drill, are wired using quick disconnects, enabling the electronics panel to be removed in transit. RAPID's and MET's wires are managed using two cable chains, one for each tool. PRISMM is powered by 120 Vac mains and incorporates the required 9 A fast-blow fuse in series along with a ground-fault circuit interrupter unit to protect operators from electrical shock. Power is then fed through a 5 V and 24 V supply to the digital components and motors.

To interface with the system, the GSC attaches using an ethernet cable plugged into a network switch. This switch then leads into two Raspberry Pis which together act as the OBC. One Raspberry Pi is responsible for communicating with the AVR microcontrollers, while the other is responsible for dealing with the video feeds from webcams. PRISMM has the capability of running two webcams and an endoscopic camera for system teleoperation and a closer view of overburden layers. The AVR microcontrollers are responsible for providing low-level communication between sensors, motors, relays, and other hardware. To communicate among each other and with the GSC, the AVR microcontrollers are connected to the Raspberry Pis via USB and provide data to the ROS network.

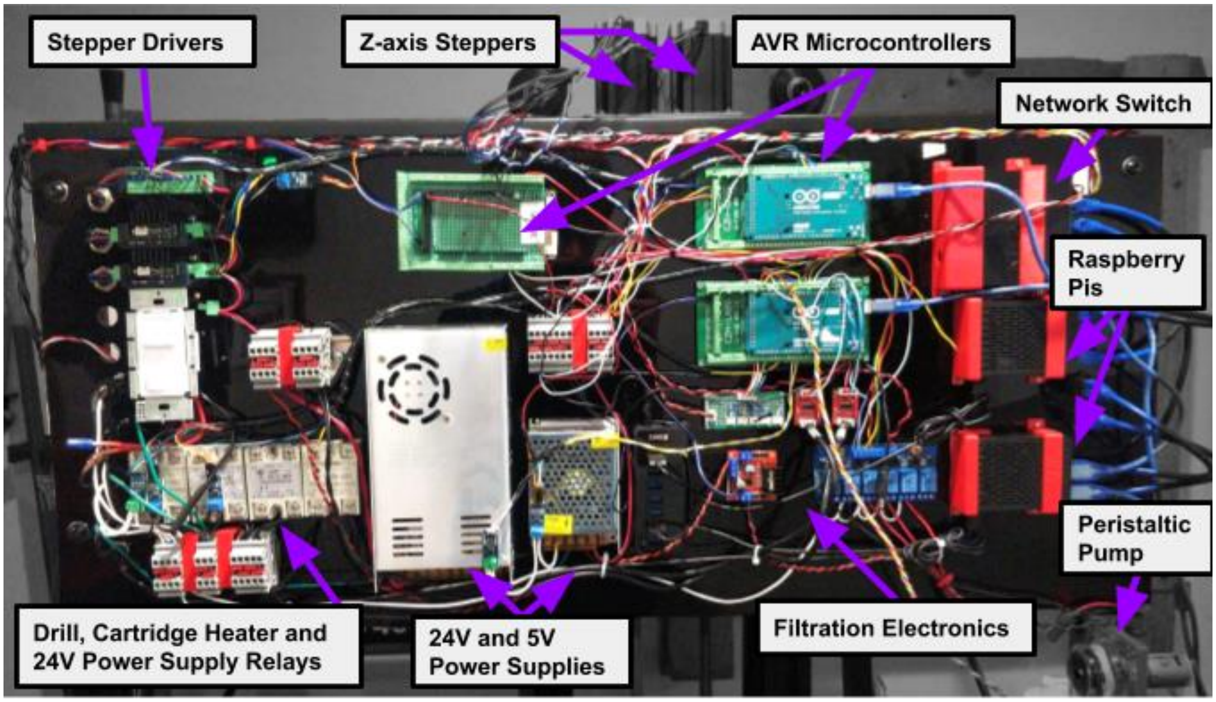

Fig. 8. *System electronics layout*

2.5.2 Software

The software and control systems of PRISMM utilize a ROS framework to facilitate communication between the various control components. Low-level control of peripherals is distributed between three AVR microcontrollers. These are responsible for all hardware interactions, control loops, and encoding/decoding messages sent across the ROS network. Each microcontroller is connected to the OBC via a USB serial connection. The OBC manages the ROS network and is responsible for video collection from the various cameras on PRISMM. Through a high-speed ethernet connection, the OBC extends the ROS network to a GSC that handles all user interfacing.

PRISMM is operated through a Qt-based user interface running on the GSC, shown in **Fig. 9**. The interface is designed to give the operator a low-level control over PRISMM's functionalities, such as individual motors and heaters. Alongside the interface, multiple terminals update the operator on the state of the device in real-time, allowing them to adapt to any emerging issues to ensure nominal performance. The GSC logs all messages sent through the ROS network. This captures the state of PRISMM's operation, which can be played back for further analysis. These logs are also crucial to creating a digital core, as they provide data that can be processed by analytical programs such as MATLAB.

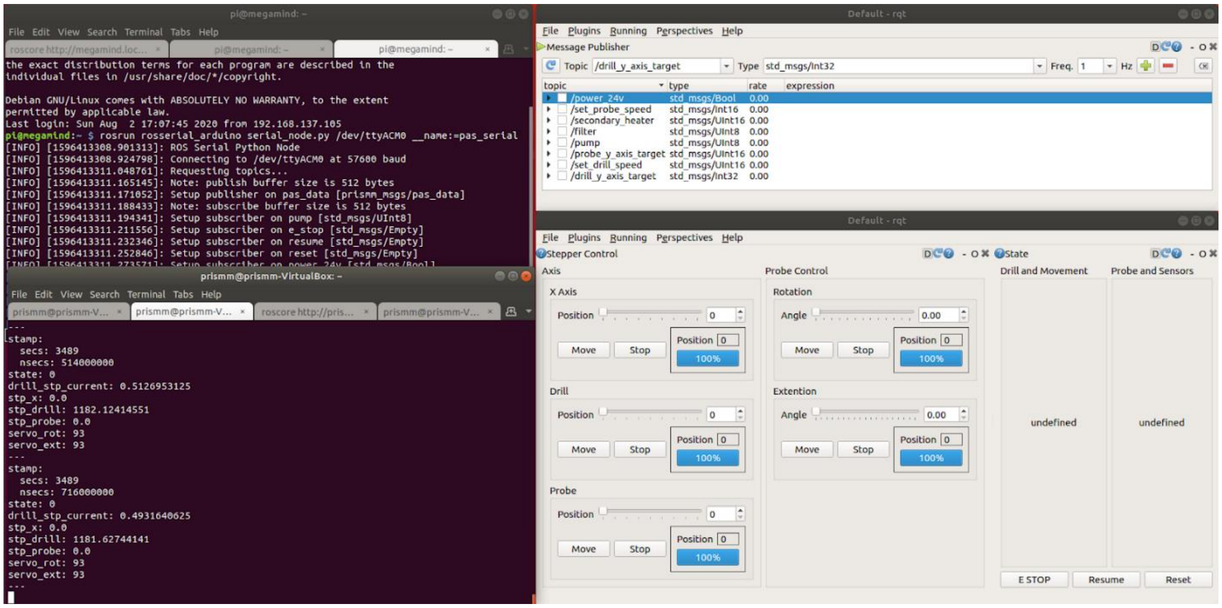

Fig. 9. *Custom UI for ROS*

2.6 Prospecting for a Digital Core

PRISMM was designed to implement pseudo-Rockwell hardness testing and HMM learning algorithms. Pseudo-Rockwell hardness testing entails pressing the drill bit into the overburden first with low force to get a baseline and then again with a higher force. Each overburden layer should have a distinct force vs. displacement graph, allowing for ranking by relative hardness. Furthermore, a HMM using depth as the time axis is employed to determine the various layers of overburden by abstracting them as states. This provides robust predictions while interpreting a drilling run by prioritizing staying in the same state over transitioning. The effectiveness of this technique is dependent on training layer data of expected materials. Unfortunately, due to the limited ability to test and gather data this year, PRISMM could not be trained with this methodology. However, the team has successfully validated these techniques in a previous year.

PRISMM is additionally capable of measuring drill current, drill stepper current, and drill r/min. Currently, these parameters can be viewed graphically by a human operator for manual digital core verification. HMM learning algorithms could be adapted to process these new metrics for further cross-corroboration. However, more testing is needed to synthesize these additions properly.

One new methodology used by PRISMM is calculating pseudo-impulse per mm of material drilled. This metric is found by taking the integral of the WOB-time graph and dividing by distance traveled. The time bounds were chosen manually from single material drilling tests. The pseudo-impulse per mm should be unique for each material and should correspond to hardness, aiding digital core generation.

3 Overall Competition Strategy

PRISMM was designed for competition efficiency by minimizing drilling and maximizing the amount of water collected from a single hole.

PRISMM begins operation by homing its vertical and horizontal axes, ensuring accurate position data for digital core creation and tool swapping. Next, a hole location is selected, and drilling commences, steadily lowering RAPID while tracking WOB, r/min, position, and time. These metrics are compared to the data collected from test runs to decipher the thickness and composition of each overburden layer. If the WOB ever surpasses 150 N, the feed rate will decrease until the WOB reaches an acceptable amount.

Similarly, the current is monitored to never exceed 9 A, pausing active drilling or melting operations if this value were approached.

Once the digital core data has registered 10 cm of ice penetrated, RAPID is retracted and the tool rack shifts until MET is aligned (**Fig. 10**). MET descends until its limit switch detects the bottom surface of the hole. The heating probe then continuously swivels and bores 18 cm deeper before beginning to articulate. As a spherical sector is melted, the extraction appendage periodically withdraws pooled water to the filtration unit where valves open as sufficient water is acquired. Once a full bowl has been created, the melting arm retracts so that the probe can bore further downwards, creating a new bowl at a greater depth.

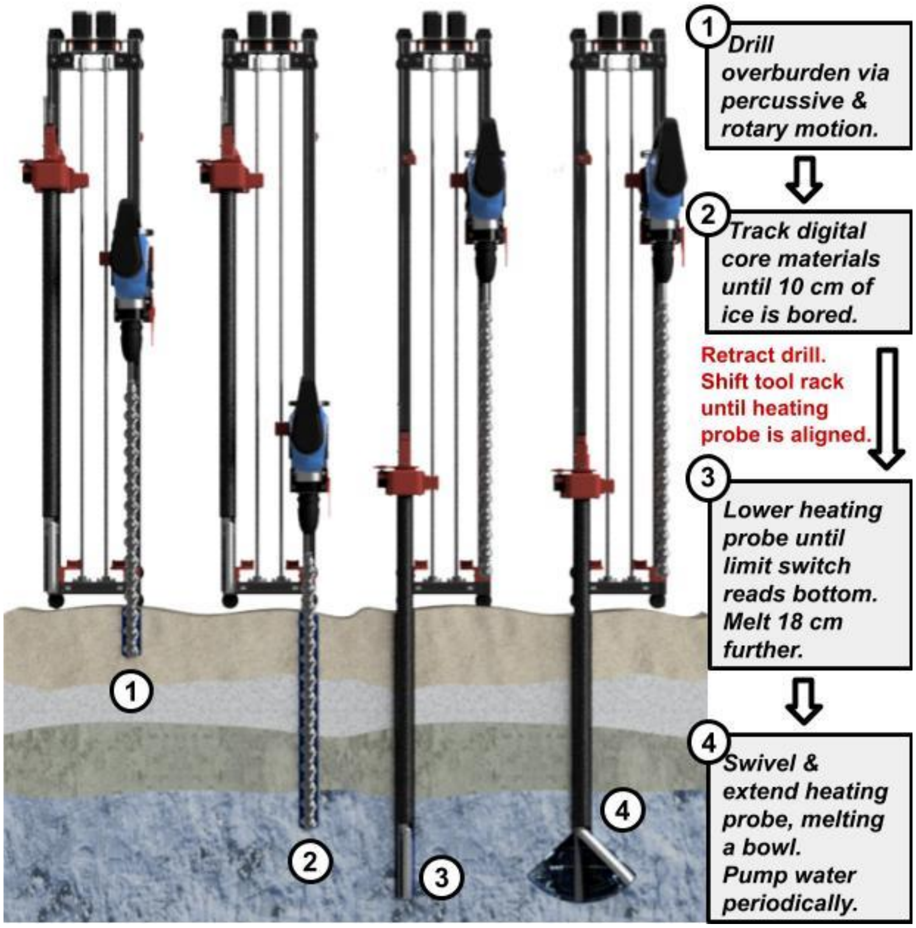

Fig. 10. *Individual bowl creation procedure*

4 Design Changes and Improvements

4.1 Drill Heating

The proposed system utilized heating elements inside the auger. This was not implemented because previous testing indicated it was unnecessary for the on-site competition due to the drill's strength and heating from friction.

4.2 MET

The heating probe had to be altered for simplified home production. All components except the melting arm were replaced with 3D printed or stock alternatives. The proposed version of MET suggested a machined extraction appendage that would include a cartridge heater to prevent freezing. This heater was removed, with the arc length of the melting arm increased to compensate. A limit switch was added to the heating probe for safe detection of the bottom surface of the hole.

4.3 Horizontal/Vertical Motion

Preliminary testing for the mid-project review highlighted several areas for improvement. The moment induced by the mass of the drilling subsystem caused the linear bearings (**Fig. 11**) to bind, preventing X-axis translation. These were swapped with roller wheels (**Fig. 12**), resulting in smooth lateral motion. The drill's Z-axis was also binding due to torque on the sliders, which was remedied using a restraint on the upper handle of the drill.

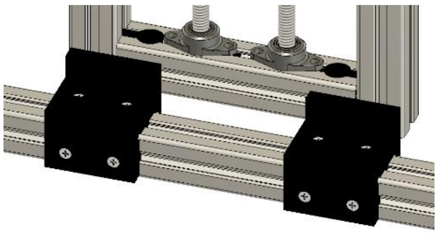

Fig. 11. *Linear bearing sliders*

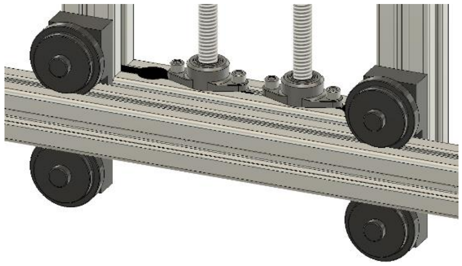

Fig. 12. *Roller wheel replacements*

4.4 Filtration

The proposed filtration system did not have a means of self-cleaning, resulting in the meshes clogging after heavy use. A new set of tubing was added, allowing the ability to purge filters and recirculate heated water. This new design dramatically extends the system lifespan before maintenance is needed.

5 Technical Specifications

Table 1. *Technical specifications*

System Mass	55.3 kg
System Volume	0.950 m x 0.956 m x 1.658 m
Length of Drill Bit	0.775 m
Maximum Weight on Bit	103 N
Rated Load	9 A
Heating Power	800 W
Max Drilling Speed	680 r/min
Torque	14.75 N·m
On-Board Computer System	Raspberry Pi 4
Communications Interface	Ethernet
Software	Robot Operating System (ROS)
Maximum Power	1080 W
System Telemetry	ROS network

6 Challenges

The team's most significant hurdle arose when in-person meetings became unsafe due to the COVID-19 pandemic. Stay-at-home orders necessitated that all subsystem progress be made individually, using only home tools and equipment. As a result, all remaining components were altered to be manufactured using 3D printing and simple hand tools or outsourced to an online machine shop service. This greatly delayed the proposed build schedule.

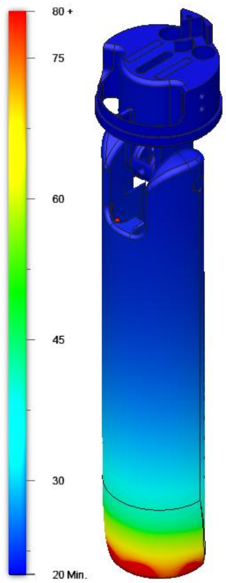

Fig. 13. *Heating probe thermal stress simulation*

Switching the design workspace from Solidworks to the cloud-based Fusion 360 allowed easier remote sharing of CAD files. In critical areas, simulations were applied to validate the function of PLA or PETG printed alternatives. The heating probe, for example, underwent thermal studies to ensure that the printed pulley and upper mount would not melt, shown in **Fig. 13**. For components with higher stresses, such as the adapters between the brass threaded nuts and load cells, static stress simulations in **Fig. 14** and **Fig. 15** confirmed that the printed substitutes could bear the same load as aluminum square tubing. While such simulations could not account for the planar layering and non-solid infill of the prints, a minimum safety factor of ten assured that no critical failures would occur. These simulations proved to be accurate, as no components during testing.

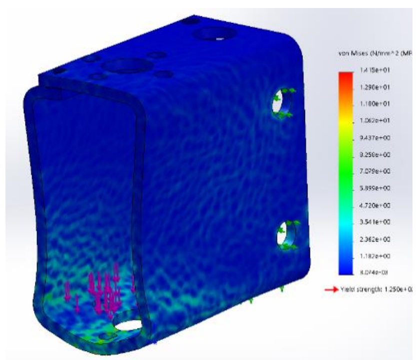

Fig. 14. *Aluminum square tubing static stress simulation*

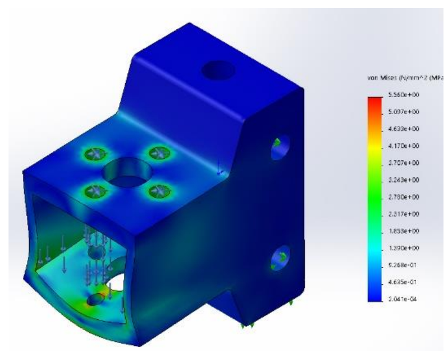

Fig. 15. *PETG print static stress simulation*

A mix of formal virtual meetings and informal working calls was essential to the team's remote coordination. Months of parallel subsystem development occurred, with the intention of safely combining once COVID-19 cases declined and teammates self-quarantined. This was finally possible in a three-day window during late July, in which all assembly, integration, wiring, and testing since the mid-point review had to occur. A viable physical prototype was completed, but limited time remained for testing and full software integration.

7 Integration & Test Plan

With only three days of in-person integration and testing, time management was crucial. The filtration subsystem and MET were developed beforehand at different homes, and software was written in advance. Wiring and debugging occurred over two days, and baseline testing was done on the third day. Tests conducted include drilling operations, using MET on a bucket of ice, and filtering water. Evaluation of RAPID consisted of penetration and data-collection of concrete and ice-cemented soil, the two materials the team anticipated being the most demanding. A melting and performance test of MET was conducted to validate its mechanical and electrical systems. MET was successfully able to rotate 360° along its central axis and articulate its melting arm. The heating probe was able to descend into the ice by continuously rotating and heating. A basic test of pumping and filtration was also conducted with the integrated system to ensure full functionality.

Basic drill telemetry data was collected during the two drilling tests that PRISMM performed. The collected data was then processed using MATLAB scripts, shown in **Fig. 16**. In testing, ice-cemented soil had a characteristic pseudo-impulse per mm of 1.73 N·s/mm, and solid concrete had a value of 1.93 N·s/mm. These two drilling tests were conducted to generate a useful baseline that could have been used during the onsite competition. The feed rate of drilling was kept constant, although concrete drilling was run at a slower feed rate.

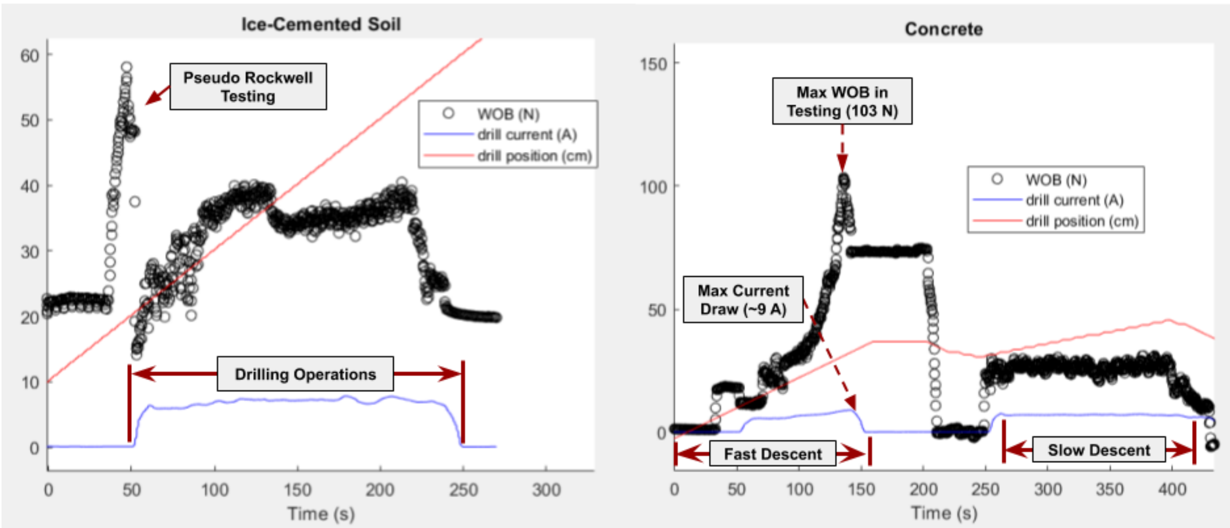

Fig. 16. *Digital core data from ice-cemented soil and concrete testing*

8 Project Timeline

In Fall 2019, the team began research for a system proposal. Since the makeup of the team was entirely first-year students, time was allotted toward studying technical and research reports to conceptualize an effective approach. In November and December, a rough CAD model was created in Solidworks, and the proposal paper was written.

After acceptance into the challenge, a timeline was developed that mapped goals up to the mid-point review. This plan had to be altered after a shipping error delayed the frame delivery by a month, and machine shop access was restricted when COVID-19 started to spread in the US. The mid-point review deadline coincided with a campus eviction, which required a total reframing of the project timeline. This was again altered as the on-site competition was pushed back to August, and ultimately canceled.

Plans were plotted in a Gantt chart via Google Sheets, with the capability to assign a task to an individual and input a completion percentage. As the competition date shifted, the Gantt chart was updated with the proper dates. An abbreviated form of this is shown in **Fig. 17**.

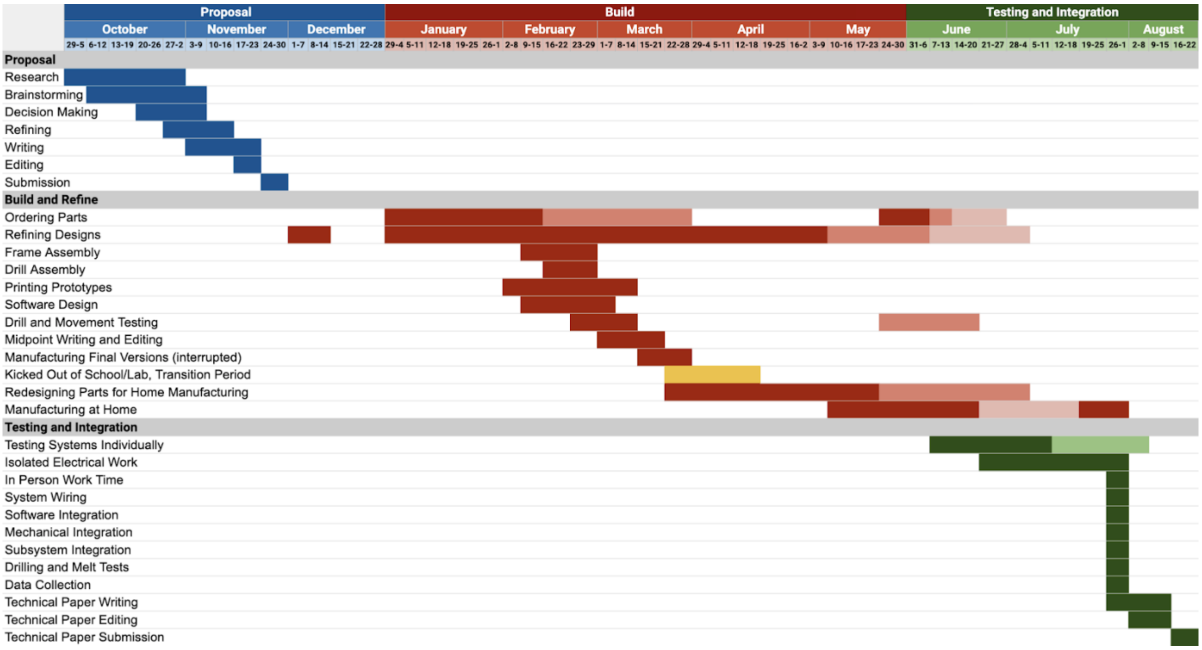

Fig. 17. *Gantt chart used for mapping progress and deadlines*

9 Tactical Plan for Contingencies

9.1 General

One of the benefits of primarily using 3D printing to construct the system is that producing backup components is inexpensive. All custom parts were designed to require little to no post-processing, making system maintenance accessible. Prior to testing, each critical component was printed with at least one replacement, which could be quickly swapped should a failure arise. Duplicates of machined components were also ordered for the melting arm and any sheet metal parts under high stress.

9.2 Translation

Each axis contains a limit switch, which allows recalibration should any debris get stuck in the channels, ensuring that the sliders never attempt to move beyond physical bounds.

9.3 Drill

Should the Hall effect sensor find that RAPID has lost rotary motion, the drill can be toggled to function only percussively. Similarly, should the load cells find that RAPID has lost percussive motion, the drill can operate solely depending on rotary motion. Both measures will require more careful descent but should be sufficient in penetrating the overburden. Additionally, both hardware and software shutoffs are available in case of any dangerous issues with the drill.

9.4 MET

The melting arm contains two thermocouples to monitor the temperature in the probe, which is vital for thermal control. This allows for redundancy in case one is lost during melting. Additionally, if data from the thermocouples is lost, the heaters will shut off until the electrical issue is addressed or the melting arm is replaced. Nearby parts with low melting points are coated in epoxy to prevent damage in the unlikely case of thermal runaway. The use of four cartridge heaters would allow for continuing viable operation if one or two were to fail.

If rotation of the carbon fiber shaft is hindered, or articulation of the melting arm fails, the system can continue to melt ice using the Rodriquez, or Rodwell method. This utilizes convection to heat a well of water, carrying the heat to the edges of the pocket to expand the well. The validity of this method was initially proven by the U.S. Army Cold Regions Research and Engineering Laboratory in the early 1960s [1] and would likely perform well given the substantial amount of heating power available. However, the extraction rate must be monitored to prevent well "collapse," which occurs when the rate of water extraction exceeds the rate of heat input necessary to maintain the liquid [2].

9.5 Filtration

Being able to recirculate water aids in removing the buildup of material around the inlet. In the case of an unremovable clog at the inlet tube of the heating probe, extraction can be manually switched to the purge tube. In the unlikely event of a total failure of the filtration chambers, indicated by the pressure gauge, the filtration system can be bypassed, and dirty water can be pumped directly into the external collection tanks.

10 Safety Plan

Table 2. *Dangers and respective precautions employed to mitigate them*

Danger	Precaution
Debris hitting operators during drilling	Operators will remain outside of a 10 ft radius during system operation. Operators will always wear eye protection.
Harmful noise when drilling	Operators will wear hearing protection.
Burns from the melting arm	An infrared thermometer will be used to check the surface temperature before any contact is attempted.
Cartridge heaters overheating	Two thermocouples located in the heating probe cut power to the cartridge heaters after detecting a thermal malfunction.
Wire entanglement	Moving wires from each tool are routed within drag chains to the frame.
Electrical dangers	Frame is grounded. All testing done with a ground-fault circuit interrupter.
Mains power	The system is turned off when wiring and grounds are used with mains. All wires are insulated.
Fumes from epoxies	All epoxying was done with an N95 mask in a well-ventilated area.
Machine shop injury	Members took a machine shop hazard course to properly handle equipment. Safety glasses are always worn when tools are in use.
COVID-19 risk	Team members must self-quarantine or be tested prior to meeting. Masks will always be worn in proximity to others.

11 Budget

Tables 3-4 contain a breakdown of the funds and resources this year's team received, as well as the areas of expense. Many electrical components were reused from previous years, minimizing the expenditure in this area. Mechanical costs surpassed their initial budget after needing to outsource machining while at home. However, considerable funds budgeted for competition travel costs remain. These will be invested in early prototyping and testing of next year's system. Additionally, two Altium licenses for custom PCB design were received-in-kind this year but will not be activated until next season.

Table 3. *Funding Received*

Funding Sources	Amount
MMIP Challenge Development Stipend 1	$5,000.00
MMIP Challenge Development Stipend 2	$5,000.00
Total	$10,000.00

Table 4. *Team expenditures*

Area	Initial Budget	Expense
Mechanical	$5,500.00	$6,102.51
Electrical	$500.00	$496.51
Travel	$3,500.00	$101.00
Testing	$500.00	$289.95
Total	$10,000	$6,989.97

12 Paths-to-flight

12.1 General Spaceflight Considerations

12.1.1 Mechanical

Weight reduction is a primary design concern for any spacefaring system, as the cost and feasibility of launches are dependent on mass. While the slotted aluminum extrusion frame met the team's needs of flexibility when prototyping, a more robust, custom frame would be implemented for a space-ready mechanism. This could be composed of a material with a higher strength-to-weight ratio, such as carbon fiber rods or titanium. Fasteners and motion components will also be minimized through design and can be made of titanium or superalloys where needed. Furthermore, all fasteners would need additional locking adhesive to withstand launch and landing vibrations, per NASA fastener requirements [3]

The drill can be customized by shifting its internal mechanisms, moving its center of mass closer to the tool rack, and by eliminating unnecessary portions of the housing.

Debris is a major concern in low-gravity environments where rubble could reach higher points of the system. To prevent such rubble from getting lodged in the system's moving parts, the lead screws and sliding joints would be sheathed within bellows.

Regardless of Lunar or Martian utilization, the system can be mounted onto a rover chassis to eliminate the need for a horizontal movement system, as shown in **Fig. 18**. As a result, the system could be stripped down to the tool rack, as well as the electronics and filtration subassemblies. This reduces the system mass by 11.5 kg and minimizes the system volume to 0.327 m x 0.379 m x 1.658 m.

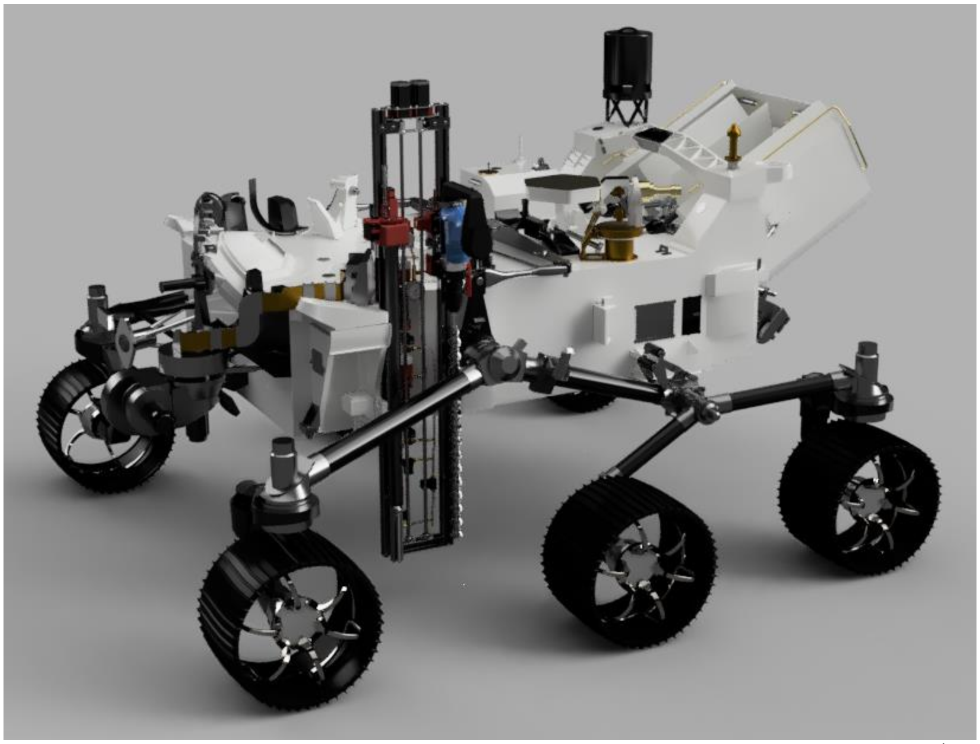

Fig. 18. *Modified PRISMM mounted onto NASA's Mars Perseverance Rover*[1]

12.1.2 Electrical

Rather than commercial computers and microcontrollers, all electronics on PRISMM would be replaced with custom electrical boards to reduce their overall footprint and weight. The electronics layout will also be optimized to allow for the shortest connections.

During launch and landing, the system will undergo extreme vibrations. Thrust oscillation produced by the launch will send waves throughout the spacecraft that can severely damage the payload if unprotected. High amplitude acoustic noise is also produced by the spacecraft's propulsion system, providing more dynamic and static stress on the craft. To avoid potential mission failure from vibration fatigue, avionics require extensive screening and qualification to be deemed flight ready. The avionics bay can be mechanically isolated through shock absorbers, with further protection provided by flexible PCBs [4]. The electrical components can also be protected using potting, where the electronic assembly is filled with a gelatinous or solid material.

The transition from PRISMM into a space-ready payload will necessitate a power source, as the system is currently powered off wall AC. A proven method employed by the Curiosity and Perseverance rovers is an onboard **r**adioisotope **t**hermoelectric **g**enerator, or RTG. This can operate without concern for sunlight and has little sensitivity to temperature and radiation [5]. However, the lifespan is relegated to the consumable plutonium. An alternative is a photovoltaic solar array, which can last over twice as long as an RTG but would limit travel into permanently shadowed regions. To bypass this, PRISMM could autonomously dock into an external power farm to recharge onboard lithium-ion batteries prior to heading on a mission.

Temperatures in space can vary from -250 °C to 280 °C or higher. In order to protect against these harsh conditions, the electronics must be in a temperature-controlled environment. A common practice to ensure safe temperatures during landing is to spray the craft with gold metal paint, preventing thermal

[1]Perseverance model obtained at https://mars.nasa.gov/resources/25042/mars-perseverance-rover-3d-model/

energy from radiating out of the craft [6]. This could be complemented by a solid silica aerogel, a highly lightweight and cost-effective insulator [7]. Heat can be diverted from the RTG to keep the electronics within their operational temperature range. The container should also feature radiators to release excess heat when the craft is experiencing temperatures higher than the preferred range.

12.2 Water Extraction on Mars

12.2.1 Mechanical

PRISMM's frame may need to be further reinforced to combat continued winds and particulate impact. All articulation points of MET would need additional dust protection to prevent binding. The heating probe could also be significantly optimized with the resources allocated to a full mission. A smaller probe diameter would enable a smaller auger diameter, in turn allowing the drill to be reduced in size, thus lowering system weight and volume.

With a combination of rover mobility and PRISMM's meter-deep reach, virtually all near-surface ice at the poles can be obtained as seen in **Fig. 19** below. Greater depths can be reached by swapping the rigid carbon fiber tube of MET with a telescoping rod and actuating the heating probe with a spooled pulley or localized motor.

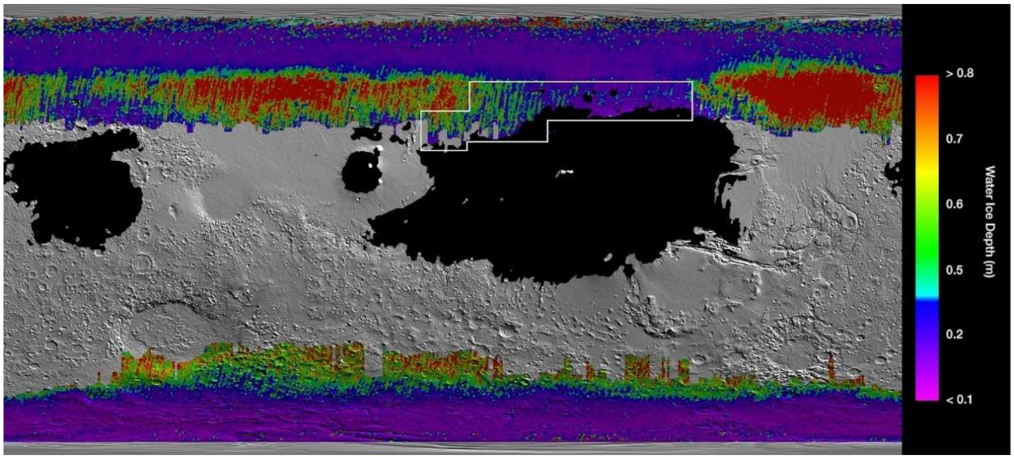

Fig. 19. *Water ice depth map on Martian terrain*
Source: [8]

Since Martian surface gravity is only 38% of Earth's, percussive drill operation may dislodge the structure from the surface and significantly impact mission performance. To combat this, PRISMM could anchor itself to the Martian surface. Alternately, if PRISMM was mounted to a rover with other systems, the added mass would likely be sufficient to prevent dislodgement.

Due to the low atmospheric pressure on Mars, ice may sublimate. To counteract this, PRISMM will need to pressurize the drilled hole while melting and extracting water. Since the boiling point of water on Mars is close to its melting point, and liquid water only exists at a small temperature interval (**Fig. 20**), MET's temperature will need to be carefully controlled.

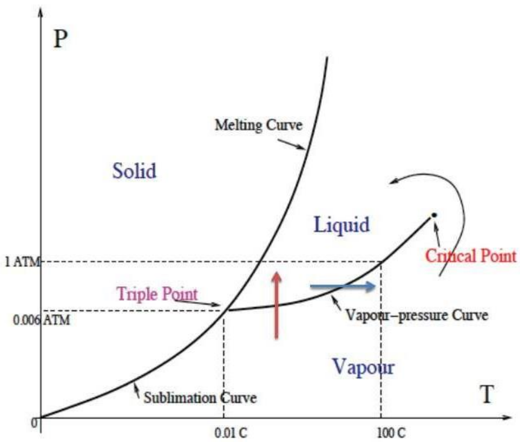

Fig. 20. *Water phase diagram on Mars*
Source: [9]

Following purification, extracted water will need to be actively heated to prevent refreezing.

Alternatively, MET can directly extract water vapor. If this approach is taken, a distillation system would be better suited than the current mesh filters, as water would not need to be boiled. Regardless of the extraction method, distillation is an ideal purification method on Mars as the pressure is low enough that this requires minimal energy and is highly sustainable.

12.2.2 Electrical

The thin atmosphere of Mars leads to a larger amount of radiation that could have devastating long-term effects on PRISMM's electronics. To counter this, a layer of aluminum or titanium shielding should be used [10]. While large amounts of radiation can be deterred with proper containment, a level of exposure will always occur, requiring all vital electronics to have backups if a failure occurs. This method has been used on previous Martian missions, resulting in an increased system lifespan [10].

Photovoltaic cells are not an ideal energy source on Mars due to the intense dust storms that block sunlight and coat panels with small electrostatic particles [11]. Additionally, no energy could be produced during a Martian night, requiring backup batteries for nighttime operation. Thus, an RTG would be better suited for its continuous and non-environmentally dependent power supply.

12.2.3 Software & Operations

A knowledgeable operator is currently required to spot developing problems and issue low-level commands. While this works well in close proximity, the inherent large latency when communicating to systems on other planets makes it difficult for an operator to react to challenges when they arise. Thus, PRISMM's software would need to carry out procedures fully autonomously and self-correct for errors. An internal model of PRISMM could be trained to detect deviations from its nominal state via routine self-diagnostics. With the addition of a rover chassis to PRISMM, additional software could be developed to autonomously determine drill sites and navigate the surface of Mars.

12.3 Lunar Prospecting

12.3.1 Mechanical

Lunar prospecting would greatly reduce the system complexity, as water collection systems such as MET, the filtration system, and their corresponding electronics will be removed.

With only 44% the gravity of Mars, there is an even greater risk of dislodgement during Lunar prospecting, necessitating an anchoring system. To ensure higher levels of autonomy are still possible, the microgravity anchoring system developed by JPL could be integrated into PRISMM. This utilizes hundreds of microspines to locate holes and divots from which the system can be anchored [12].

12.3.3 Software & Operations

While one-way transmissions can take multiple minutes to get to Mars, the Earth's closer proximity to the moon minimizes such latency to just over a second. This allows a broader range of capabilities, as the craft would not be limited by autonomy. As mentioned prior, several systems will be removed for lunar prospecting. This will simplify control software.

Since prospecting is a higher priority on the moon, a more advanced digital core system could be implemented. This system would employ a larger range of sensors, such as radar thickness sensors. Such non-contacting electromagnetic sensors were developed by the U.S. Bureau of Mines to measure the thickness of coal deposits but were found to be able to determine the thickness and locations of other features such as concrete or steel beams [13]. By employing such a technique, it would be possible to determine both thickness and other useful information such as the dielectric constant of the lunar surface.
Adding more sensors would bring the added complexity of more data, which could be handled by utilizing a predictive model to determine overburden makeup. This model could be trained on Earth using simulated regolith and other known materials to accurately determine the composition of different layers below the lunar surface.

References

[1] D. Marquis, "ERDC supports NASA's mission to Mars", *Engineer Research and Development Center*, 2020. [Online]. Available: https://www.erdc.usace.army.mil/Media/News-Stories/Article/2301946/erdc-supports-nasas-mission-to-mars/.

[2] S. Hoffman, A. Andrews and K. Watts, *"Mining" Water Ice on Mars*. 2016. [Online]. Available: https://www.nasa.gov/sites/default/files/atoms/files/mars_ice_drilling_assessment_v6_for_public_release.pdf

[3] *Requirements for Threaded Fastening Systems in Spaceflight Hardware*. Washington DC: NASA, 2012.

[4] R. Caimi, R. Margashayam, J. Nayfeh, and K. Thompson, "NASA Technical Reports Server (NTRS)," NASA, 01-Jan-2001. [Online]. Available: https://ntrs.nasa.gov/citations/20010038008. [Accessed: 16-Aug-2020].

[5] "Radioisotope Thermoelectric Generators (RTGs) | Cassini – NASA Solar System Exploration", *NASA Solar System Exploration*, 2018. [Online]. Available: https://solarsystem.nasa.gov/missions/cassini/radioisotope-thermoelectric-generator/.

[6] "The Rover's Temperature Controls," NASA. [Online]. Available: https://mars.nasa.gov/mer/mission/rover/temperature/. [Accessed: 16-Aug-2020].

[7] "The Rover's Temperature Controls", *Mars.nasa.gov*. [Online]. Available: https://mars.nasa.gov/mer/mission/rover/temperature/#aerogel.

[8] "NASA's Treasure Map for Water Ice on Mars", *NASA*, 2019. [Online]. Available: https://www.nasa.gov/feature/jpl/nasas-treasure-map-for-water-ice-on-mars.

[9] S. Giorgini, *Phase diagram of water*. 2016.

[10] Tran, L., 2019. *How NASA Prepares Spacecraft For The Harsh Radiation Of Space*. [online] NASA. Available at: <https://www.nasa.gov/feature/how-nasa-prepares-spacecraft-for-the-harsh-radiation-of-space/>.

[11] K. Mersmann, "The Fact and Fiction of Martian Dust Storms", *NASA*, 2015. [Online]. Available: https://www.nasa.gov/feature/goddard/the-fact-and-fiction-of-martian-dust-storms.

[12] A. Parness, M. Frost and J. King, *Microgravity Drill and Anchor System*. Pasadena: NASA Tech Briefs, 2013.

[13] R. Chufo, *An Electromagnetic Noncontacting Sensor for Thickness Measurement in a Dispersive Medium*. Pittsburgh: NASA, 1994.

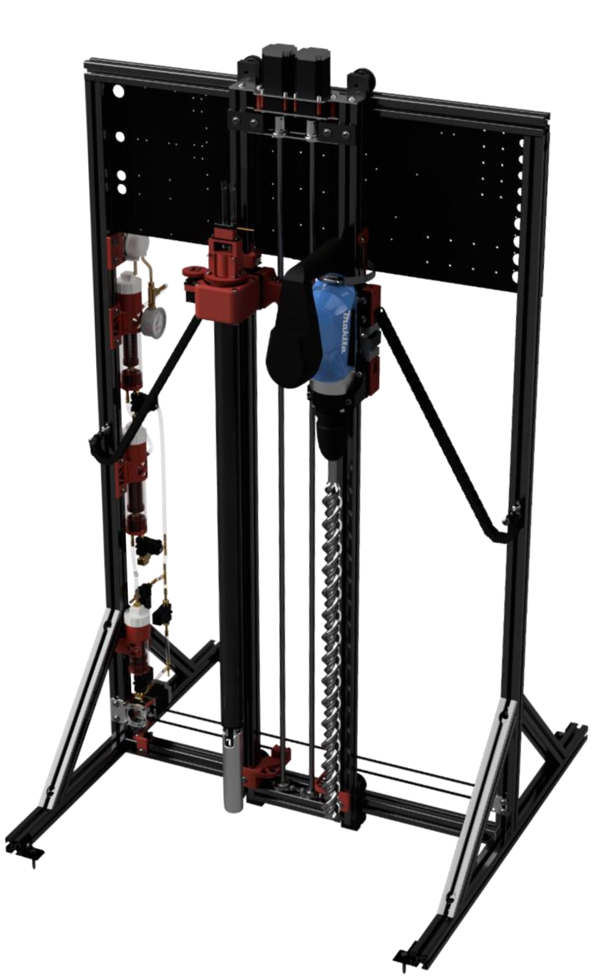

Final CAD Render	*Final Physical Assembly*